nature cell biology

AMPK controls the speed of microtubule polymerization and directional cell migration through CLIP-170 phosphorylation

Atsushi Nakano[1,4], Hisakazu Kato[3,4], Takashi Watanabe[5,6], Kyung-Duk Min[1,3], Satoru Yamazaki[1], Yoshihiro Asano[3,4], Osamu Seguchi[1], Shuichiro Higo[3], Yasunori Shintani[3], Hiroshi Asanuma[1], Masanori Asakura[1], Tetsuo Minamino[3], Kozo Kaibuchi[6], Naoki Mochizuki[2], Masafumi Kitakaze[1] and Seiji Takashima[3,4,7]

AMP-activated protein kinase (AMPK) is an energy-sensing Ser/Thr protein kinase originally shown to be regulated by AMP[1]. AMPK is activated by various cellular stresses that inhibit ATP production or stimulate ATP consumption[2]. In addition to its role in metabolism, AMPK has recently been reported to reshape cells by regulating cell polarity and division[3–6]. However, the downstream targets of AMPK that participate in these functions have not been fully identified. Here, we show that phosphorylation of the microtubule plus end protein CLIP-170 by AMPK is required for microtubule dynamics and the regulation of directional cell migration. Both inhibition of AMPK and expression of a non-phosphorylatable CLIP-170 mutant resulted in prolonged and enhanced accumulation of CLIP-170 at microtubule tips, and slower tubulin polymerization. Furthermore, inhibition of AMPK impaired microtubule stabilization and perturbed directional cell migration. All of these phenotypes were rescued by expression of a phosphomimetic CLIP-170 mutant. Our results demonstrate, therefore, that AMPK controls basic cellular functions by regulating microtubule dynamics through CLIP-170 phosphorylation.

Besides the metabolic activity of AMPK, there is growing evidence that AMPK and its upstream kinase liver kinase B1 (LKB1) have pivotal roles in the establishment of cell polarity and cell division[7,8] in *Drosophila melanogaster*[6,9] and *Caenorhabditis elegans*[10]. In mammalian cells, AMPK is associated with tight junction assembly, and regulates epithelial polarity[3,4].

To discover previously unidentified substrates of AMPK, we performed a unique screen using two-step column chromatography combined with an *in vitro* kinase reaction. Using mouse heart homogenates, we purified and identified a cytoplasmic linker protein CLIP-170, which has a relative molecular mass of 170,000 (M_r 170K) and is a substrate of AMPK (Supplementary Information, Fig. S1). CLIP-170 is one of the microtubule plus end proteins originally identified as proteins that bind endocytic vesicles to microtubules[11,12]. CLIP-170 directly binds freshly polymerized distal ends of growing microtubules and rapidly dissociates from the older microtubule lattice[13]. However, a direct link between CLIP-170 and physiological control of cell function has not been fully elucidated. Both recombinant AMPK made by 293T cells and AMPK purified from rat liver efficiently phosphorylated recombinant CLIP-170 (Fig. 1a). Phospho amino acid analysis revealed that AMPK phosphorylates a Ser residue of CLIP-170 (Fig. 1b). A combination of mass spectrometric and multiple mutation analyses of CLIP-170 identified Ser 311 as the only AMPK phosphorylation site. AMPK did not phosphorylate CLIP-115, a close mammalian homologue of CLIP-170, or Ser 737 of CLIP-170, demonstrating an AMPK substrate consensus sequence[14] (Fig. 1c). Recombinant glutathione S-transferase (GST)-fused wild-type CLIP-170 and a Ser 311-to-Ala mutant (S311A) of CLIP-170 were produced in *Escherichia coli*. The wild-type, but not the S311A mutant, was phosphorylated by AMPK and 0.29 mole of phosphate per mole of CLIP-170 was incorporated, indicating that Ser 311 of CLIP-170 is phosphorylated directly by AMPK (Fig. 1d). Next, we generated an antibody against Ser 311-phosphorylated CLIP-170 (p-CLIP-170). The specificity and sensitivity of this antibody were confirmed by the following observations: first the p-CLIP-170 antibody exclusively detected p170 as a single band, even when total cell lysates were assessed; and second, it did not recognize phosphatase-treated p170 (Fig. 1e). Analyses using this antibody also demonstrated the specific phosphorylation of CLIP-170 at Ser 311 by AMPK (Fig. 1f). The amino acid sequence surrounding Ser 311 matches the consensus sequence of a potential AMPK phosphorylation site and is well conserved among various species (Fig. 1g).

[1]Division of Cardiovascular Medicine, National Cardiovascular Center and [2]Department of Structural Analysis, National Cardiovascular Center, Research Institute Suita, Osaka 565-8565, Japan. [3]Department of Cardiovascular Medicine and [4]Department of Molecular Cardiology, Osaka University Graduate School of Medicine Suita, Osaka 565-0871, Japan. [5]Institute for Advanced Research, Nagoya University Graduate School of Medicine and [6]Department of Cell Pharmacology, Nagoya University Graduate School of Medicine, Nagoya, Aichi 466-8550, Japan.
[7]Correspondence should be addressed to S.T. (e-mail: takasima@medone.med.osaka-u.ac.jp)

Received 4 March 2010; accepted 29 April 2010; published online 23 May 2010; DOI: 10.1038/ncb2060

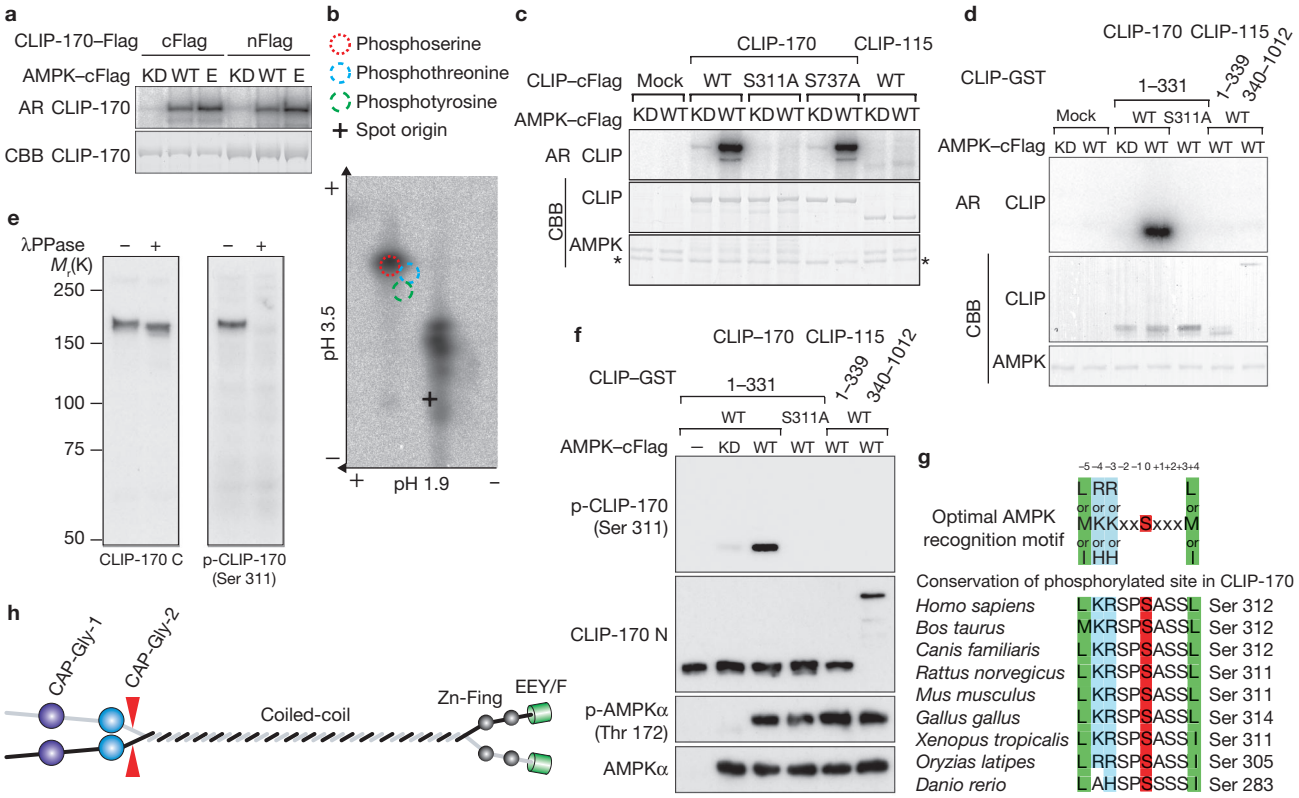

Figure 1 *In vitro* phosphorylation of CLIP-170 Ser311 by AMPK. (**a**) An autoradiographic (AR) image of mammalian recombinant carboxy-terminally (cFlag) or amino-terminally (nFlag) Flag-tagged CLIP-170 incubated with either recombinant kinase dead (KD), wild-type (WT) or endogenous (E) AMPK. (**b**) Phospho-amino acid analysis of CLIP-170 phosphorylated by AMPK. Only a Ser residue was phosphorylated (radioactivity indicated by the red circle). (**c**) An AR of mammalian recombinant cFlag-tagged CLIP-170 (WT, S311A and S737A) and CLIP-115 (WT) incubated with recombinant KD or WT AMPK. AMPK is indicated by an asterisk. (**d**) An AR image of GST fusion proteins representing amino acids 1–331 of CLIP-170 (WT or S311A), or either the N (1–339) or the C (340–1012) terminus of CLIP-115 incubated with KD or WT AMPK. (**e**) Lysate of Vero cells treated with or without phosphatase (λPPase) was subjected to immunoblot analysis with an antibody against the C terminus of CLIP-170 (CLIP-170 C) and a Ser 311 phosphospecific antibody (p-CLIP-170). (**f**) Immunoblot analysis of the GST-fused CLIP constructs described above with KD or WT AMPK. These samples were blotted using a p-CLIP-170 and a non-phosphospecific antibody against the N terminus of CLIP-170 (CLIP-170 N). CLIP-170 N also recognized CLIP-115. (**g**) The optimal AMPK recognition motif. The consensus sequence of AMPK is identical to the sequence around Ser 311 of CLIP-170. This residue is highly conserved among various species. (**h**) Structural model of CLIP-170. Ser 311 is located between the CAP-Gly-2 domain and the coiled-coil region in CLIP-170. Ser 311 is indicated by red arrowheads. CAP-Gly, cytoskeleton-associated protein Gly-rich; Zn-Fing, C-terminal zinc knuckle of CLIP-170; EEY/F, C-terminal amino sequence of CLIP-170; CBB, Coomassie brilliant blue staining. Uncropped images of blots are shown in Supplementary Information, Fig. S5.

Ser 311 is located between a Gly-rich microtubule-binding domain (cytoskeleton-associated protein Gly-rich; CAP-Gly) and a coiled-coil domain (Fig. 1h).

Next, we examined AMPK-induced CLIP-170 phosphorylation in cultured cells. Compound C, an inhibitor of AMPK, reduced the phosphorylation level of CLIP-170 (Fig. 2a), whereas the AMPK activator AICAR (5-aminoimidazole-4-carboxyamide ribonucleoside) did not affect CLIP-170 phosphorylation (Supplementary Information, Fig. S2a). The phosphorylation level of acetyl-CoA carboxylase (ACC), which was used as a control, reflected the conventional responses of cells to both Compound C and AICAR. Although Compound C is an inhibitor of AMPK, it can also inhibit several other kinases[15]. Therefore, we used short interfering RNAs (siRNAs) to specifically deplete AMPK. Depletion of AMPK with siRNAs specific for either the α_1 or the α_2 catalytic subunit also reduced CLIP-170 phosphorylation (Fig. 2b). These data indicate that phosphorylation of CLIP-170 at Ser 311 is regulated endogenously by AMPK. To explore the significance of AMPK-induced CLIP-170 phosphorylation, we first immunocytochemically investigated the localization of phosphorylated CLIP-170 in cultured cells. A non-phospho-specific antibody (CLIP-170 C), as well as a Ser 311 phospho-specific antibody (p-CLIP-170), stained the plus ends of microtubules (Fig. 2c, d). To distinguish between the total CLIP-170 population and phosphorylated CLIP-170, Vero cells stably expressing CLIP-170–EGFP were stained with these antibodies. The pattern observed with the CLIP-170 C antibody (red or yellow) completely matched that of CLIP-170–EGFP (Fig. 2e, green), suggesting that CLIP-170–EGFP mimics the localization of endogenous CLIP-170. By contrast, p-CLIP-170 staining mostly overlapped with CLIP-170–EGFP but was located predominantly on the distal side (red or yellow) of CLIP-170–EGFP (Fig. 2f, green). This result suggests that phosphorylated CLIP-170 attaches to microtubules at the more distal end, compared with non-phosphorylated CLIP-170. A marked change in CLIP-170 localization was observed when these cells were treated with Compound C: CLIP-170–EGFP accumulated significantly farther along the length of the microtubules (Fig. 2g, h, green). CLIP-170 C staining again overlapped with CLIP-170–EGFP (Fig. 2g, red or yellow), whereas p-CLIP-170 staining was markedly reduced and localized as only a tiny

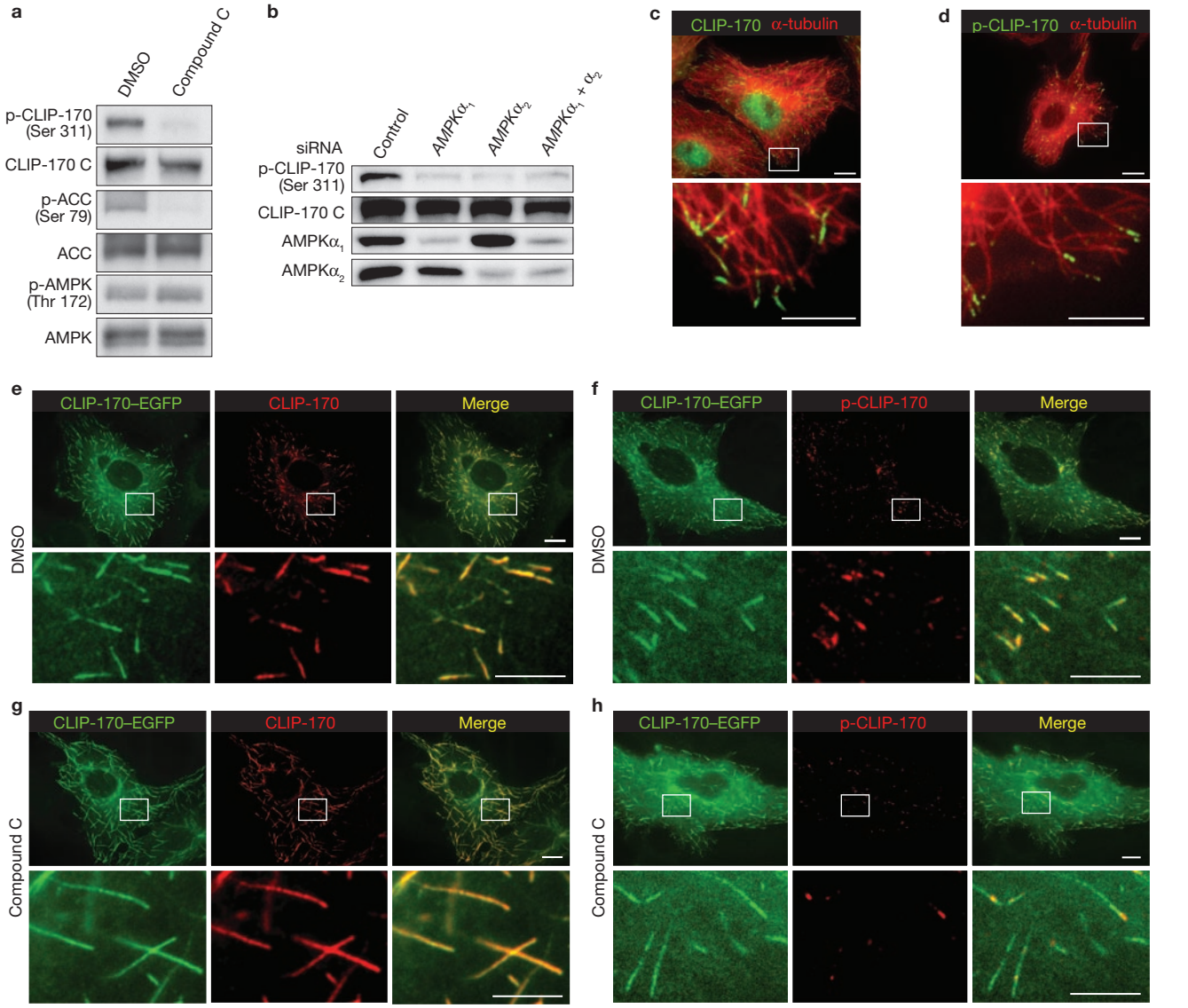

Figure 2 CLIP-170 phosphorylated by AMPK localizes to microtubule tips. (**a**) Immunoblot analysis of the phosphorylation level of CLIP-170, AMPK, and ACC in cells treated with 0.2% DMSO or Compound C (20 μM). CLIP-170 C is a non-phosphospecific antibody that recognizes the C terminus of CLIP-170. (**b**) Immunoblot analysis of the phosphorylation level of CLIP-170 and the expression level of AMPKα$_1$ and α$_2$ in cells treated with siRNA targeting *AMPKα$_1$*, *α$_2$*, or both subunits of AMPK. (**c**) Immunostained images of Vero cells stained with anti-α-tubulin and the anti-CLIP-170 C antibodies. (**d**) Immunostained images of Vero cells stained with α-tubulin and p-CLIP-170 antibodies. (**e**, **f**) Immunostained images of Vero cells stably expressing CLIP-170–EGFP (GFP image, left) and treated with DMSO as a control. These cells were stained with a CLIP-170 C antibody (**e**, centre) or a p-CLIP-170 antibody (**f**, centre). (**g**, **h**) Immunostained images of Vero cells stably expressing CLIP-170–EGFP (GFP image, left) and treated with Compound C. These cells were stained with a CLIP-170 C antibody (**g**, centre) or a p-CLIP-170 antibody (**h**, centre). The merged images of each panel are shown on the right. The white boxed regions in the panels are enlarged below each panel. Scale bars, 10 μm (**c**–**h**, upper rows) and 5 μm (**c**–**h**, bottom rows). Uncropped images of blots are shown in Supplementary Information, Fig. S5.

spot within the CLIP-170–EGFP-positive region (Fig. 2h, red or yellow). Most of the CLIP-170 on microtubules, therefore, was non-phosphorylated, and a small amount of phosphorylated CLIP-170 accumulated at the distal ends. To examine the precise distribution of CLIP-170 on the microtubules under AMPK-inhibited conditions, linescan analysis along the microtubules was performed using double immunocytochemistry with CLIP-170 C and tubulin antibodies. We separately measured total CLIP-170 associated with microtubule plus ends, and CLIP-170 associated with the outermost microtubule tips (within a 0.129-μm square box at the very end of the microtubules). When compared with the DMSO control Compound C treatment increased the association of CLIP-170 with microtubules both in the whole tip (6-fold) and at the outer tip (1.7-fold) (Supplementary Information, Fig. S2b–d). Depletion of both AMPKα$_1$ and α$_2$ by siRNA also resulted in accumulation of CLIP-170 on microtubule plus ends, similarly to inhibition by Compound C (Supplementary Information, Fig. S2e, f). This characteristic change of CLIP-170 localization prompted us to examine the role of AMPK in the regulation of microtubule dynamics.

To study how AMPK regulates microtubule dynamics, we examined the behaviour of CLIP-170 in living cells. First, we tested whether phosphorylation levels of CLIP-170 affected polymerization of microtubules.

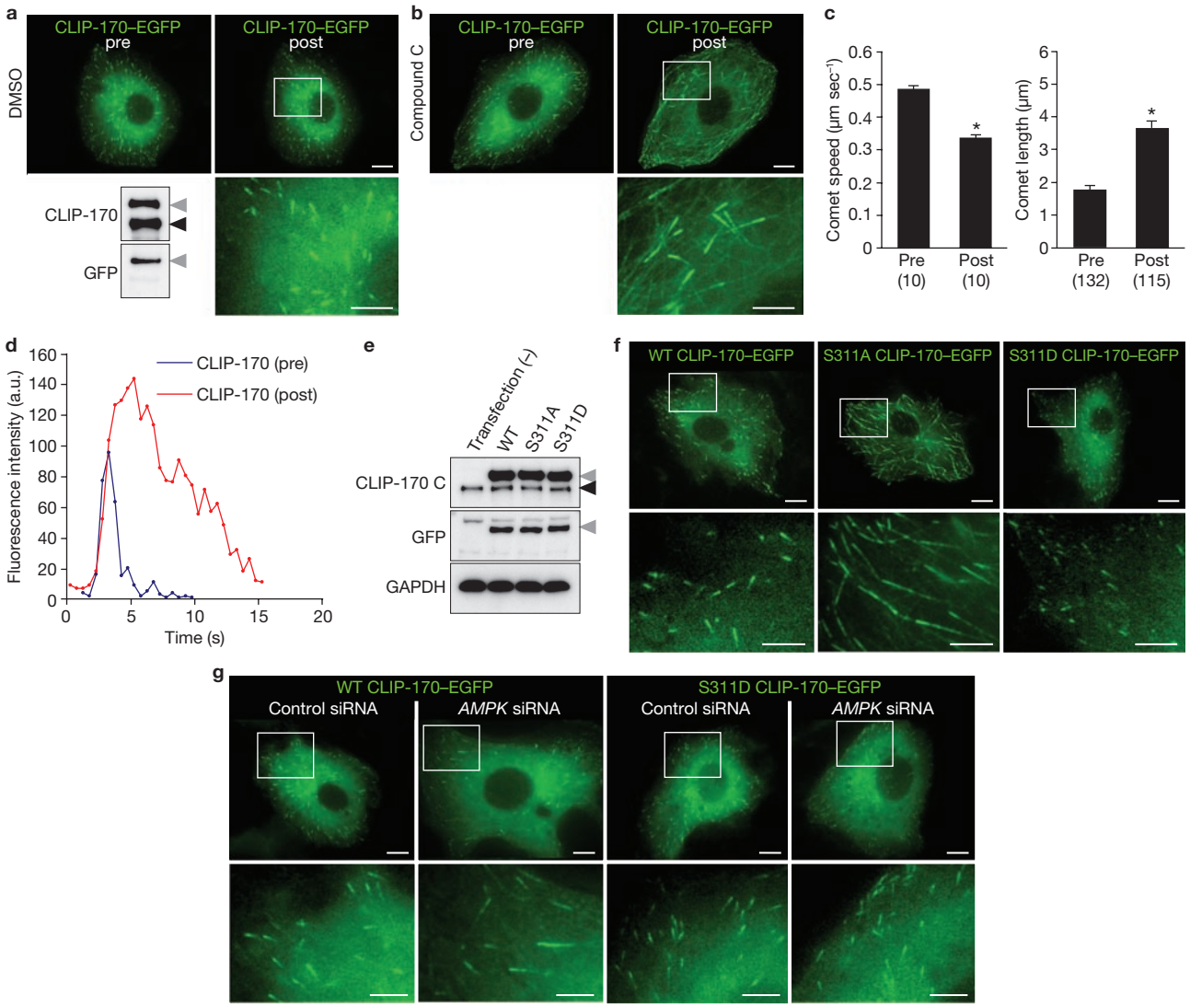

Figure 3 AMPK-phosphorylated CLIP-170 regulates microtubule dynamics. (**a**, **b**) GFP images of Vero cells stably expressing CLIP-170–EGFP before (pre) and 10 min after (post) treatment with 0.2% DMSO control (**a**) or Compound C (20 μM, **b**). The immunoblot on the left shows exogenous CLIP-170–EGFP (grey arrowheads) and endogenous CLIP-170 (black arrowhead). (**c**) Bar graphs showing the speed (left panel) and length (right panel) of a single comet before (pre) and 10 min after (post) Compound C treatment in the same cell. Values are means ± s.e.m.; *n* shown in parentheses; $*P<0.01$, compared with pre. (**d**) Fluorescence intensity plots of CLIP-170–EGFP of the same cell before (pre, blue) and 10 min after (post, red) Compound C treatment. (**e**) Expression levels of wild-type (WT), S311A and S311D CLIP-170–EGFP in transiently transfected Vero cells were comparable, as determined by immunoblotting using the antibodies indicated on the left. The grey and black arrowheads indicate GFP-tagged exogenous CLIP-170 and endogenous CLIP-170, respectively. (**f**) GFP images of cells transiently expressing WT (left), S311A (centre) and S311D (right) CLIP-170–EGFP. (**g**) GFP images of the cells transiently expressing WT and S311D CLIP-170–EGFP treated with control siRNA or siRNA targeting both *AMPK*α_1 and α_2. White boxed regions in the panels are enlarged below each panel. Scale bars, 10 μm (**a**, **b**, **f**, **g**, upper panels) and 5 μm (**a**, **b**, **f**, **g**, enlarged images). Uncropped images of blots are shown in Supplementary Information, Fig. S5.

By live-cell imaging, we observed that stably expressed CLIP-170–EGFP accumulated at the distal ends of microtubules and seemed to move like a comet from the centrosome to the cell periphery (as shown in sequential images converted to video, Supplementary Information, Movie 1). The speed of the CLIP-170 comets coincided with that of microtubule polymerization[16,17]. Consistent with our results in fixed cells (Fig. 2), 10-min inhibition of AMPK by Compound C in living cells also resulted in elongated CLIP-170 comets, compared with control DMSO-treated cells (Fig. 3a–c). Moreover, the speed of the comets was reduced by Compound C (Fig. 3c; Supplementary Information, Movie 2). To analyse the CLIP-170 behaviour more precisely, we measured the fluorescence intensity values along the CLIP-170–EGFP tracks over time in the same living cells before and 10 min after Compound C treatment. This fluorescence intensity analysis of CLIP-170–EGFP demonstrated that Compound C markedly increased the peak fluorescence intensity and slowed the dissociation of CLIP-170 from the older part of the microtubules (Fig. 3d). Using the same cell line stably expressing CLIP-170–EGFP, depletion of AMPK by siRNA also reduced the speed of the comets and increased the length of CLIP-170 comets (Supplementary Information, Fig. S2g–i, Movie 3). To elucidate the specific role of CLIP-170 Ser 311 phosphorylation by AMPK, we compared the phenotypes of cells transiently transfected with wild-type and two Ser 311 mutants of CLIP-170. S311A CLIP-170–EGFP

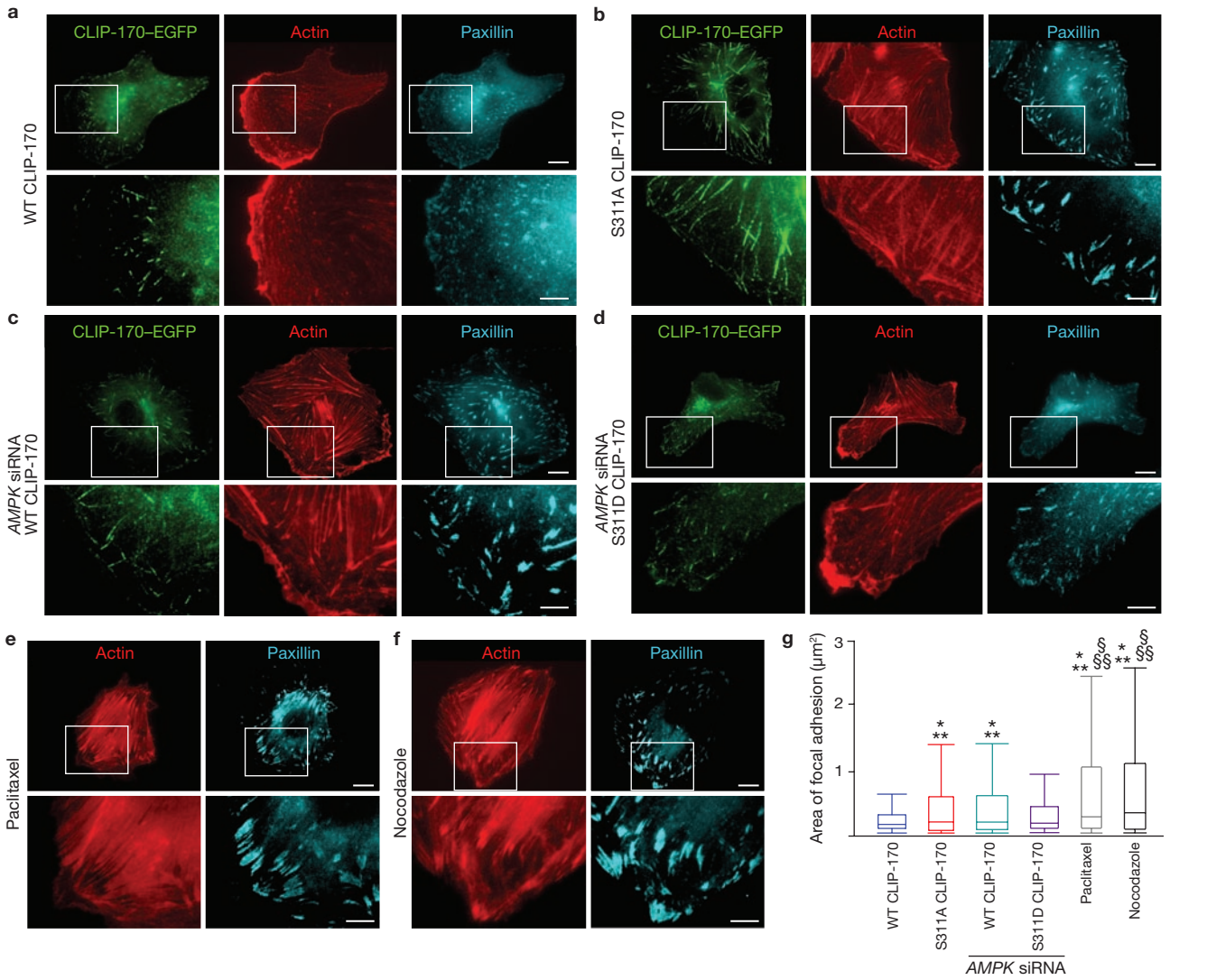

Figure 4 Loss of CLIP-170 phosphorylation increases the size of focal adhesions. (**a**, **b**) Immunostained images of Vero cells transiently expressing wild-type (WT; **a**) and S311A (**b**) CLIP-170–EGFP (GFP image, left). These cells were stained with fluorescein-conjugated phalloidin (centre) and a paxillin antibody (right) to visualize actin microfilaments and focal adhesions, respectively. (**c**, **d**) Immunostained images of Vero cells transiently expressing WT (**c**) and S311D (**d**) CLIP-170–EGFP (GFP image, left) treated with siRNA targeting both *AMPK*α_1 and α_2. These cells were stained with fluorescein-conjugated phalloidin (centre) and a paxillin antibody (right). (**e**, **f**) Immunostained images of Vero cells treated with 5 μM paclitaxel (**e**) or 10 μM nocodazole (**f**). These cells were stained with fluorescein-conjugated phalloidin (left) and a paxillin antibody (right). The white boxed regions in the panels are enlarged below each panel. Scale bars, 10 μm (**a**–**f**, upper row) and 5 μm (**a**–**f**, bottom row). (**g**) Box and whisker plots of the area stained with a paxillin antibody showing the 25th percentile (bottom line of each box), median (middle line of each box), 75th percentile (top line of each box), and the 5th and 95th percentiles (each whisker); $n = 10$ for each group; $^{*}P < 0.01$, compared with WT CLIP-170; $^{**}P < 0.01$, compared with S311D CLIP-170 treated with *AMPK* siRNA; $^{§}P < 0.01$, compared with S311A CLIP-170; $^{§§}P < 0.01$, compared with WT CLIP-170 treated with *AMPK* siRNA.

is a non-phosphorylatable mutant, and a Ser 311-to-Asp mutant (S311D CLIP-170–EGFP) is a phosphomimetic mutant. These EGFP fusion proteins were equally expressed in Vero cells (Fig. 3e). S311A CLIP-170–EGFP accumulated as comets with longer tails and moved more slowly than wild-type CLIP-170–EGFP (Fig. 3f centre; Supplementary Information, Table S1, Movie 4). By contrast, S311D CLIP-170–EGFP had the same comet length and moved with the same speed as wild-type CLIP-170–EGFP (Fig. 3f, right; Supplementary Information, Table S1, Movie 5). These findings are consistent with the observation that most of the endogenous CLIP-170 was phosphorylated by AMPK. Furthermore, S311D CLIP-170–EGFP rescued the phenotypes caused by siRNA depletion of AMPK (Fig. 3g; Supplementary Information, Table S1, Movie 6). Also, in the cells treated with Compound C, transfection of S311D CLIP-170–EGFP restored comet speed and length. Quantitative data of comet speed and length in various conditions are summarized in Supplementary Information, Table S1.

CLIP-170 binds only to the growing phase of microtubules. To further examine microtubule dynamics during the shortening phase, Vero cells stably expressing α-tubulin–EGFP were observed before and 10 min after Compound C treatment. Compound C markedly decreased the microtubule shortening distance (Supplementary Information, Fig. S2j, Movie 7). This change in microtubule behaviour may stabilize microtubules. We then observed microtubule stability by staining them with an antibody against detyrosinated tubulin (Glu tubulin,

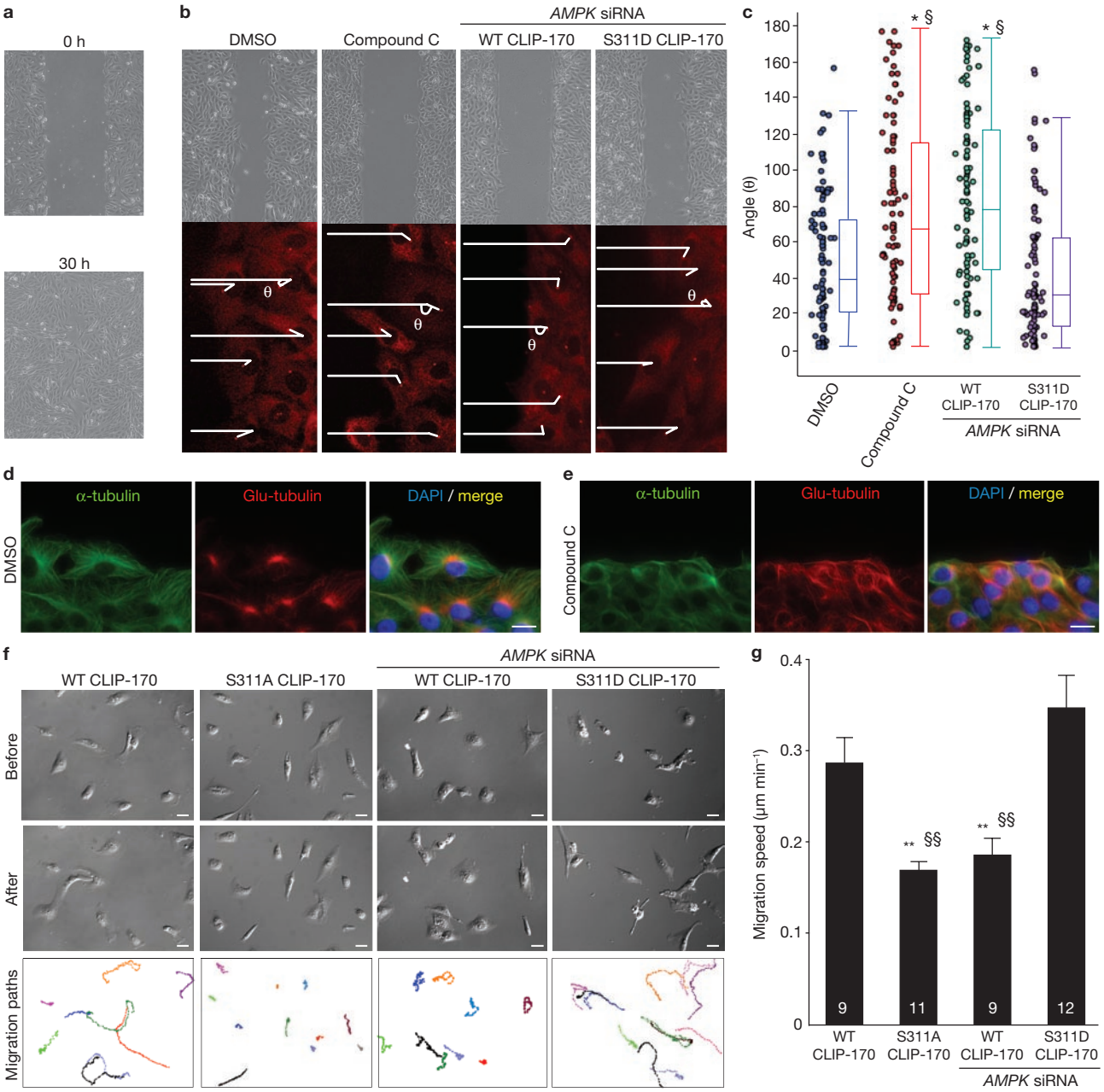

Figure 5 Phosphorylation of CLIP-170 at Ser 311 is essential for cell polarity and directional cell migration. (**a**) Phase contrast microscopy images of Vero cells before (upper panel) and 30 h after (lower panel) scratch. (**b**) Phase contrast microscopy images (upper panels) and immunostained images of Vero cells stained with a γ-tubulin antibody (lower panels) after being subjected to a scratch assay. Images were captured 12 h after incubation. The cells were treated by either repeated administration of DMSO control or Compound C, or transiently transfected with wild-type (WT) or S311D CLIP-170 and siRNA targeting both *AMPKα*$_1$ and α_2. To assess cell polarity, the angles (θ) between the lines of γ-tubulin and the scratched line at the centre of each nucleus were measured as a marker for MTOC reorientation (lower panels). (**c**) Box and whisker plots of angles (θ) with actual data points shown on the left; n=100 per group; $^*P$ <0.01, compared with DMSO; $^{\S}P$ <0.01, compared with S311D CLIP-170 treated with *AMPK* siRNA. (**d**, **e**) Images of Vero cells immunostained with an α-tubulin (left, green) and a detyrosinated (Glu) tubulin antibody (centre, red) after being subjected to a scratch assay following repeated treatment with control DMSO (**d**) or Compound C (**e**) for 6 h. DAPI stained nucleus (blue). The merged images of each panel are shown on the right. Scale bars, 20 μm. (**f**) Time lapse images acquired by differential interference contrast of cells transiently expressing WT, S311A, and WT or S311D CLIP-170 treated with siRNA targeting both *AMPKα*$_1$ and α_2. Images acquired before (upper line of each panel) and after 12 h (middle line of each panel) are shown. The bottom row of each panel shows the individual paths of migrating cells over 12 h. Scale bars, 30 μm. (**g**) Bar graphs showing the migration speed of the cells from (**f**); Numbers in the bars indicate n. Values represent means ± s.e.m; $^{**}P$ <0.01, compared with WT CLIP-170. $^{\S\S}P$ <0.01, compared with S311D CLIP-170 treated with *AMPK* siRNA.

named for the newly exposed C-terminal glutamate residue). The amount of stable microtubules was greater in cells transiently expressing S311A CLIP-170–EGFP (Supplementary Information, Fig. S3b) than in cells transiently expressing wild-type CLIP-170 (Supplementary Information, Fig. S3a). Cell depleted of AMPK by siRNA (Supplementary Information, Fig. S3g), or treated with Compound C (Supplementary

Information, Fig. S3d) also showed the same phenotype as cells expressing S311A CLIP-170. These phenotypes were rescued by S311D CLIP-170 (Supplementary Information, Fig. S3f, i). Collectively, these data suggest that phosphorylation of CLIP-170 at Ser 311 by AMPK is necessary for proper CLIP-170 dissociation from microtubules, and that this modification of CLIP-170 is essential for efficient polymerization and depolymerization of microtubules. Dynamic modulation of microtubule polymerization and stability by AMPK-phosphorylated CLIP-170 might represent a previously unknown mechanism through which AMPK establishes cell polarity. Therefore, we further examined the role of CLIP-170 phosphorylation by AMPK during cell polarization and subsequent cell migration.

During cell migration, microtubules target focal adhesions and regulate cell–extracellular matrix (ECM) adhesion[18–20]. Thus, we first examined whether phosphorylation of CLIP-170 at Ser 311 affects the size of focal adhesions. Isolated Vero cells transiently expressing wild-type CLIP-170–EGFP formed an actin meshwork in protruding lamellipodium. Furthermore, staining focal adhesions with a paxillin antibody revealed small, scattered spots located predominantly at the protruding lamellipodium (Fig. 4a). By contrast, expression of S311A CLIP-170–EGFP caused loss of lamellipodium formation and adhesion maturation, which resulted in significantly enlarged spots (Fig. 4b). Similar phenotypes were observed when AMPK was depleted by siRNA (Fig. 4c) or inhibited by Compound C (Supplementary Information, Fig. S4b). These AMPK depletion phenotypes were almost completely rescued by the expression of S311D CLIP-170–EGFP (Fig. 4d, g; Supplementary Information, Fig. S4d). Treatment with paclitaxel and nocodazole (Fig. 4e, f), both of which disturb microtubule dynamics, resulted in similar phenotypes of abnormal size of focal adhesion as cells expressing S311A CLIP-170–EGFP and cells depleted of AMPK. These data indicate that AMPK-dependent phosphorylation of CLIP-170 regulates the size of focal adhesions by regulating microtubule dynamics. The fact that inhibiting AMPK-induced phosphorylation of CLIP-170 altered the size of focal adhesions and lamellipodium formation suggests an important role of the AMPK–CLIP-170 signalling axis in cell polarity and migration. We examined the effect of AMPK inhibition on cell polarity using the scratch assay. The leading cells started to polarize and migrated towards a scratched line, closing the gap in about 30 h (Fig. 5a). However, repeated treatment with Compound C and depletion of AMPK by siRNA both inhibited closure of the gap and interfered with microtubule-organizing centre (MTOC) reorientation in leading cells. Expression of S311D CLIP-170 rescued AMPK depletion (Fig. 5b, c; Supplementary Information, Fig S4g, h). The first two layers of the leading cells showed that the stabilized microtubules stained with a detyrosinated (anti-Glu) tubulin antibody were clearly polarized towards the leading edge (Fig. 5d). By contrast, AMPK inhibition by Compound C increased the amount of stable microtubules, which lost their orientation towards the leading edge (Fig. 5e). Finally, we tested the effect of CLIP-170 phosphorylation on free cell migration. Wild-type CLIP-170-expressing cells migrated with active lamellipodium formation. By contrast, S311A CLIP-170-expressing cells and wild-type CLIP-170-expressing cells treated with *AMPK* siRNA showed diminished migration and fewer membrane extensions (Fig. 5f). Again, expression of S311D CLIP-170 rescued the effect of siRNA *AMPK* knockdown of (Fig. 5g; Supplementary Information, Movie 8). These data suggest that AMPK-induced phosphorylation of CLIP-170 is required to establish front–rear polarity and proper cell migration, presumably through the regulation of microtubule tip dynamics.

We have shown here that CLIP-170 is a strong candidate AMPK substrate that regulates cell polarity through alteration of its dynamics on the plus ends of microtubules. Recently, abnormal mitotic phenotypes were observed for both *AMPK*- and *LKB1*-null *Drosophila*. They demonstrated that AMPK phosphorylates myosin regulatory light chain (MRLC) directly, and a phosphomimetic MRLC transgene rescued the polarity phenotypes induced by loss of the AMPK pathway[6]. However, the transgene did not rescue all phenotypes, suggesting that AMPK signalling is mediated by additional downstream targets.

The dynamics of CLIP-170 on microtubules were recently and precisely investigated both *in vitro* and *in vivo*[13,17]. In these reports, CLIP-170 turnover on microtubules was rapid, and the diffusion of CLIP-170 was rate-limiting for its binding to microtubule plus ends. They also showed that the ends of growing microtubules contain a surplus of sites to which CLIP-170 can bind, and the older lattice has a lower affinity for CLIP-170 than the newer, growing ends of the microtubules. These changes in the affinity of plus end proteins for microtubules may be essential for their effects on microtubule dynamics.

We could not demonstrate an altered affinity of phosphorylated CLIP-170 for the microtubule plus end *in vitro* because of the difficulty associated with reconstituting the plus end as *in vivo*. However, we speculate, for the following reasons, that non-phosphorylated CLIP-170 increased its affinity to microtubules. First, linescan analysis showed that depletion of AMPK activity increased the association not only of total CLIP-170 with the microtubule but also of CLIP-170 at the outer tip. Second, the fluorescence intensity analysis measured in living cells indicated that non-phosphorylated CLIP-170 increased the peak fluorescence intensity and slowed its dissociation from the plus end of microtubules. Third, phosphorylated CLIP-170 localized within the more distal portion of the total CLIP-170 population. These results support the hypothesis that the phosphorylation status of CLIP-170 at Ser 311 determines its affinity for microtubules. Because CLIP-170 turnover on microtubules is rapid, phosphorylation may be a suitable modification to regulate its affinity for microtubules. We conclude that phosphorylation of CLIP-170 alters its affinity for microtubule plus ends and that this phenomenon might contribute to the rapid turnover of CLIP-170, which is necessary for efficient microtubule polymerization.

The observation that the phosphorylation status of CLIP-170 regulates the growth rate of microtubules has not been reported. The precise mechanisms remain unclear; however we speculate that Ser 311 phosphorylation is necessary to reduce the affinity of CLIP-170 for the microtubule lattice and promote the efficient turnover of CLIP-170 at the plus end, similarly to a microtubule polymerase.

Another intriguing phenotype of AMPK depletion is the marked enhancement of microtubule stabilization in migrating cells. Moreover, AMPK depletion impaired the polarized stabilization of microtubules towards the leading edge. AMPK depletion not only reduced the speed of polymerization but also decreased the shortening distance of microtubules. Because both phenomena prolong the lifetime of microtubules, these two changes might cause the ubiquitous enhancement of microtubule stabilization.

Expression of the non-phosphorylatable CLIP-170 S311A mutant and depletion of AMPK disrupted front–rear polarity and reduced cell migration. The precise mechanisms of this phenotype are unclear, but decreased

microtubule polymerization and unpolarized microtubule stabilization might affect the function of microtubules, which are required to establish cell polarity. We have shown that inhibiting CLIP-170 phosphorylation resulted in significant enlargement of focal adhesions, as detected with a paxillin antibody. Enlarged focal adhesions are similar to the phenotype observed in cells treated with paclitaxel or nocodazole, both of which disrupt microtubule dynamics. Microtubules bind to paxillin and help the cell adhesion system to destabilize focal adhesions and promote cell motility[21,22]. These functions suggest that microtubules play a key part in cell polarity and migration through interactions with focal adhesion molecules. Taken together, the results suggest that AMPK promotes the appropriate formation of focal adhesions, the subsequent establishment of cell polarity, and directional cell migration through efficient polymerization of microtubules, by phosphorylating CLIP-170 at Ser 311.

Under normal cell culture conditions, neither enhanced activation of AMPK by AICAR nor S311D CLIP-170–EGFP altered microtubule dynamics, indicating a high basal phosphorylation of CLIP-170. This might be caused by a high affinity of AMPK for CLIP-170, or colocalization of AMPK and CLIP-170.

The results of our broad substrate screening method suggest that CLIP-170 is one of the most important substrates of AMPK in various organs. We believe that observing microtubule dynamics is necessary to evaluate multiple functions of AMPK. Also, similarly to paclitaxel or nocodazole treatment, strong inhibition of microtubule dynamics by the CLIP-170 S311A mutant may have clinical implications. The interaction between AMPK and CLIP-170 might be a therapeutic target for treatment of conditions such as cancer, tumour angiogenesis and neointimal hyperplasia. □

METHODS

Methods and any associated references are available in the online version of the paper at http://www.nature.com/naturecellbiology/

Note: Supplementary Information is available on the Nature Cell Biology website.

ACKNOWLEDGEMENTS

We thank M. Amano and S. Fukuhara for helpful discussions, and M. Koyama (Olympus Corporation) for technical advice regarding microscopy. This research was supported by: a Grants-in-Aid from the Ministry of Health, Labour and Welfare of Japan; Grants-in-Aid from the Ministry of Education, Culture, Sports, Science and Technology of Japan; grants from the Japan Heart Foundation; grants from the Japan Cardiovascular Research Foundation; a grant from the Japan Society for the Promotion of Science; a grant from the Mochida Memorial Foundation for Medical and Pharmaceutical Research; and a Grant-in-Aid from the Japan Medical Association.

AUTHOR CONTRIBUTIONS

A.N. designed and conducted the study, performed most of the experiments, and wrote the manuscript; S.T. designed and conducted the study, performed the biochemical experiments and wrote the manuscript; H.K. carried out immunoblot analysis; K.M. independently counted the number of cells; S.Y. helped to generate the plasmids; Y.A., O.S., S.H., Y.S., H.A., M.A. and T.M. discussed the results and reviewed the manuscript; T.W. and K.K. generated and provided antibodies and Vero cells and reviewed the manuscript; N.M. conducted and supported the biological experiments and wrote the manuscript; M.K. supervised all work.

COMPETING FINANCIAL INTERESTS

The authors declare no competing financial interests.

Published online at http://www.nature.com/naturecellbiology/
Reprints and permissions information is available online at http://npg.nature.com/reprintsandpermissions/

1. Yeh, L. A., Lee, K. H. & Kim, K. H. Regulation of rat liver acetyl-CoA carboxylase. Regulation of phosphorylation and inactivation of acetyl-CoA carboxylase by the adenylate energy charge. *J. Biol. Chem.* **255,** 2308–2314 (1980).
2. Hardie, D. G. AMP-activated/SNF1 protein kinases: conserved guardians of cellular energy. *Nature Rev. Mol. Cell Biol.* **8,** 774–785 (2007).
3. Zhang, L., Li, J., Young, L. H. & Caplan, M. J. AMP-activated protein kinase regulates the assembly of epithelial tight junctions. *Proc. Natl Acad. Sci. USA* **103,** 17272–17277 (2006).
4. Zheng, B. & Cantley, L. C. Regulation of epithelial tight junction assembly and disassembly by AMP-activated protein kinase. *Proc. Natl Acad. Sci. USA* **104,** 819–822 (2007).
5. Mirouse, V., Swick, L. L., Kazgan, N., St. Johnston, D. & Brenman, J. E. LKB1 and AMPK maintain epithelial cell polarity under energetic stress. *J. Cell Biol.* **177,** 387–392 (2007).
6. Lee, J. H. *et al.* Energy-dependent regulation of cell structure by AMP-activated protein kinase. *Nature* **447,** 1017–1020 (2007).
7. Williams, T. & Brenman, J. E. LKB1 and AMPK in cell polarity and division. *Trends Cell Biol.* **18,** 193–198 (2008).
8. Jansen, M., Ten Klooster, J. P., Offerhaus, G. J. & Clevers, H. LKB1 and AMPK family signaling: the intimate link between cell polarity and energy metabolism. *Physiol. Rev.* **89,** 777–798 (2009).
9. Martin, S. G. & St. Johnston, D. A role for *Drosophila* LKB1 in anterior–posterior axis formation and epithelial polarity. *Nature* **421,** 379–384 (2003).
10. Watts, J. L., Morton, D. G., Bestman, J. & Kemphues, K. J. The *C. elegans par-4* gene encodes a putative serine-threonine kinase required for establishing embryonic asymmetry. *Development* **127,** 1467–1475 (2000).
11. Rickard, J. E. & Kreis, T. E. Identification of a novel nucleotide-sensitive microtubule-binding protein in HeLa cells. *J. Cell Biol.* **110,** 1623–1633 (1990).
12. Pierre, P., Scheel, J., Rickard, J. E. & Kreis, T. E. CLIP-170 links endocytic vesicles to microtubules. *Cell* **70,** 887–900 (1992).
13. Dragestein, K. A. *et al.* Dynamic behavior of GFP-CLIP-170 reveals fast protein turnover on microtubule plus ends. *J. Cell Biol.* **180,** 729–737 (2008).
14. Hardie, D. G., Carling, D. & Carlson, M. The AMP-activated/SNF1 protein kinase subfamily: metabolic sensors of the eukaryotic cell? *Annu. Rev. Biochem.* **67,** 821–855 (1998).
15. Bain, J. *et al.* The selectivity of protein kinase inhibitors: a further update. *Biochem. J.* **408,** 297–315 (2007).
16. Perez, F., Diamantopoulos, G. S., Stalder, R. & Kreis, T. E. CLIP-170 highlights growing microtubule ends *in vivo*. *Cell* **96,** 517–527 (1999).
17. Bieling, P. *et al.* CLIP-170 tracks growing microtubule ends by dynamically recognizing composite EB1/tubulin-binding sites. *J. Cell Biol.* **183,** 1223–1233 (2008).
18. Wu, X., Kodama, A. & Fuchs, E. ACF7 regulates cytoskeletal-focal adhesion dynamics and migration and has ATPase activity. *Cell* **135,** 137–148 (2008).
19. Rodriguez, O. C. *et al.* Conserved microtubule–actin interactions in cell movement and morphogenesis. *Nat. Cell Biol.* **5,** 599–609 (2003).
20. Small, J. V., Geiger, B., Kaverina, I. & Bershadsky, A. How do microtubules guide migrating cells? *Nature Rev. Mol. Cell Biol.* **3,** 957–964 (2002).
21. Turner, C. E. Paxillin and focal adhesion signalling. *Nat. Cell Biol.* **2,** E231–E236 (2000).
22. Broussard, J. A., Webb, D. J. & Kaverina, I. Asymmetric focal adhesion disassembly in motile cells. *Curr. Opin. Cell Biol.* **20,** 85–90 (2008).

METHODS

Reagents and antibodies. The following reagents were purchased: Compound C (Calbiochem); AMPK (Upstate); DAPI (Molecular Probes); AICAR (5-aminoimidazole-4-carboxyamide ribonucleoside; Cell Signaling) and Geneticin (Invitrogen). Generation of a CLIP-170 C (1:2,000 dilution for immunoblot; 1:200 dilution for immunostain) and a CLIP-170 N (1:4,000 dilution) antibody was described previously[23]. The detyrosinated (Glu) tubulin antibody (1:400 dilution) was a gift from G. G. Gundersen[24]. The remaining antibodies purchased were: anti-AMPKα, AMPKα$_1$, AMPKα$_2$, phospho-Thr 172 AMPKα, ACC and phospho-Ser 79 ACC antibodies (each 1:200 dilution; Cell Signaling); anti-paxillin antibody (1:200 dilution, Zymed Laboratories); anti-α-tubulin (1:400) and γ-tubulin antibodies (1:500 dilution; Sigma-Aldrich); anti-GFP antibody (1:2,500 dilution; Chemicon); anti-GAPDH (glyceraldehyde-3-phosphate dehydrogenase) antibody (1:5,000 dilution; Chemicon); horseradish peroxidase–coupled sheep anti-rabbit and anti-mouse IgG (Cappel); and Alexa Fluor 350-, Alexa Fluor 488- and Alexa Fluor 568-labelled secondary antibodies and Alexa Fluor 555-conjugated phalloidin (each 1:500 dilution; Molecular Probes).

Generation of polyclonal antibodies specific for the pS311 of CLIP-170. A phospho-specific polyclonal antibody to CLIP170 (Ser 311) was generated as follows. Ser-phosphorylated and non-phosphorylated peptides corresponding to CLIP170 amino acid sequences S311 (amino acids 305–316, SLKRSP(pS) ASSLS) were synthesised. Rabbits were immunized 5 times with the keyhole limpet hemocyanin–phosphopeptide conjugates mixed with Freund's complete adjuvant, and bled 7 days after the last immunisation. Phosphopeptide-reactive antibody was captured by a column containing phosphopeptide-conjugated sepharose. The antibody was then eluted, and those reactive to sequences other than phosphoserine were removed using a column containing non-phosphorylated peptides. Specific reactivity with the targeted phosphoserine sequence was confirmed by an ELISA in which phosphorylated and non-phosphorylated peptides were coated.

Plasmids. A set of cDNA fragments encoding rat AMPKα$_1$ (NM_019142), full-length mouse CLIP-170 and amino acids 1–331 of mouse CLIP-170 (BC007191), as well as full-length mouse CLIP-115 and amino acids 1–339 and 340–1012 of CLIP-115 (NM_009990) were PCR amplified from rat and mouse heart cDNA libraries and inserted into pENTR/D-TOPO vectors (pENTR-WT AMPKα$_1$, pENTR-WT CLIP-170, pENTR-WT CLIP-170 1–331, pENTR-WT CLIP-115, pENTR-WT CLIP-115 1-339, and pENTR-WT CLIP-115 340–1012) using Gateway Technology (Invitrogen). The kinase- dead (KD) AMPKα$_1$ (a Thr 172 Ala mutant) was generated by PCR using pENTR-WT AMPKα1 as a template and the following primers: 5′-TTTTTAAGAGCTAGCTGTGGCTCGCC-3′ and 5′-GCCACAGCTAGCTCTTAAAAATTCAC-3′. S311A and S737A CLIP-170 were also generated by PCR using pENTR-WT CLIP-170 as a template and the following primer pairs: forward 5′-CGAAGCCCTGCTGCCTCCTCCCTCAGCTCCATGAGC-3′ and reverse 5′-GGAGGAGGCAGCAGGGCTTCGCTTCAGGCTGGCGGGCG-3′ and forward 5′-AAAGCCAATGCCGAAGGTAAACTGGAGCTCGAGACACTTA-3' and reverse 5′-TTTACCTTCGGCATTGGCTTTCCGAAGCGCATCAAGATCC-3′, respectively (underlined nucleotides indicate mutated sites). To prepare Flag-tagged protein, pENTR-WT AMPKα$_1$, pENTR-KD AMPKα$_1$, pENTR-WT CLIP-170, pENTR-S311A CLIP-170, pENTR-S737A CLIP-170, and pENTR-WT CLIP-115 were subcloned into pEF-DEST51/cFlag vectors (yielding pEF-DEST51-WT AMPKα$_1$, pEF-DEST51-KD AMPKα$_1$, pEF-DEST51-WT CLIP-170, pEF-DEST51-S311A CLIP-170, pEF-DEST51-S737A CLIP-170, and pEF-DEST51-WT CLIP-115, respectively) or a pcDNA3.1/nFlag–DEST vector (pcDNA3.1-WT CLIP-170) using the Gateway system. To prepare the GST fusion protein, pENTR-WT CLIP-170 1–331, pENTR-WT CLIP-115 1–339, and pENTR-WT CLIP-115 340–1012 were subcloned into pDEST15 vectors (pDEST15-WT CLIP-170 1–331, pDEST15-WT CLIP-115 1–339, and pDEST15-WT CLIP-115 340–1012, respectively) using the Gateway system. The pEGFP–CLIP-170 construct was produced as described by Fukata *et al.*[23]. Mutant CLIP-170 constructs in which Ser 311 was replaced with Ala or Asp were generated by PCR using pEGFP–CLIP-170 as the template and the following primers: Ala forward 5′-CGCAGCCCTGCTGCCTCTTCCCTCAGCTCCATGAGC-3′ and reverse 5′-GGAAGAGGCAGCAGGGCTGCGCTTCAGGCTGGCGGACG-3′ and Asp forward 5′-CGCAGCCCTGATGCCTCTTCCCTCAGCTCCATGAGC-3′ and reverse 5′-GGAAGAGGCATCAGGGCTGCGCTTCAGGCTGGCGGACG-3′ (underlined nucleotides indicate mutated sites).

Cell culture, plasmid transfection, and siRNAs. The 293T cells were obtained from the American Type Culture Collection. Preparation of Vero cells and generation of Vero cells stably expressing CLIP-170–EGFP or tubulin–EGFP were performed as described by Fukata *et al.*[23]. All cells were maintained in Dulbecco's modified Eagle's medium (Sigma-Aldrich) supplemented with 10% foetal calf serum (Equitech-Bio) at 37°C in a 5% CO_2 atmosphere at constant humidity. Vero cells stably expressing CLIP-170–EGFP were selected in the presence of geneticin (1.5 mg ml^{-1}). Vero and 293T cells were transfected with plasmids using Lipofectamine 2000 reagent (Invitrogen), according to the manufacturer's protocol. To knock down *AMPK*, Vero cells were transfected with of siRNAs (50 nmol l^{-1}) targeting *AMPKα$_1$* (sense: gaggagagcuauuugauuaTT; antisense: uaaucaaauagcucuccucTT) and *AMPKα$_2$* (sense: gcuguuugguguagguaaaTT; antisense: uuuaccuacaccaaacagcTT) (B-Bridge International) using Lipofectamine 2000, according to the manufacturer's protocol. As a negative control, siControl (B-Bridge International) was used. After incubation with siRNAs for 40 h, the cells were analysed. When we used cells transiently transfected CLIP-170–EGFP mutant, we screened the cells by the expression level of each CLIP-170–EGFP protein by measuring the total fluorescence intensity of EGFP throughout the whole cell with background subtraction. Then we selected the cells expressing similar amount of CLIP-170–EGFP proteins for assay when we compared the dynamics of each CLIP-170 transfectant.

Animals. Female C57BL/6J mice (Japan animals, Osaka, Japan) were used in the study. All procedures conformed to the *Guide for the Care and Use of Laboratory Animals* (NIH publication no. 85-23, revised 1996) and were approved by the Osaka University Committee for Laboratory Animal Use.

Protein purification. Recombinant Flag-tagged AMPK, CLIP-170, and CLIP-115 proteins were purified as follows: 293T cells transfected with pEF-DEST51/cFlag plasmid encoding WT or KD AMPKα$_1$, WT, S311A and S737A CLIP-170 and WT CLIP-115 were lysed in lysis buffer A (20 mM MOPS, pH 7.4, 10% glycerol, 0.15 M NaCl, 1% CHAPS, 1 mM EDTA, protease inhibitor cocktail (Nacalai Tesque), 50 mM β-glycerophosphate, 25 mM NaF, and 1 mM Na_3VO_4) and immunoprecipitated with anti-Flag M2 agarose (Sigma) at 4°C for 1 h. The beads were washed three times with lysis buffer A and eluted with elution buffer (20 mM Tris-HCl, pH 7.4, 10% glycerol, 0.3 mM NaCl, 0.1% CHAPS, 0.5 mg ml-1 Flag peptide (Sigma), and 1 mM dithiothreitol (DTT)) at 4°C for 1 h. After centrifugation, the supernatants were used as recombinant Flag-tagged proteins. Recombinant CLIP-170–GST and CLIP-115–GST proteins were purified as follows: BL21-AI chemically competent *E. coli* (Invitrogen) were transformed with a DEST15 plasmid encoding WT CLIP-170 1–331, WT CLIP-115 1–339, or WT CLIP-115 340–1012, and induced with 0.02% L-arabinose (Sigma) at 20°C for 12 h. The cells were collected by centrifugation and lysed by sonication in phosphate-buffered saline (PBS) containing 5 mM EDTA and protease inhibitor cocktail. After addition of 1% Triton X-100, the cell lysates were agitated at 4°C for 30 min and pulled down with glutathione sepharose 4 Fast Flow (GE Healthcare) at 4°C for 1.5 h. After being washed three times, the proteins were eluted with 10 mM reduced glutathione and ultrafiltrated in elution buffer using a Nanosep 10K Device (Pall Life Science).

Screening for AMPK substrates. Organs obtained from C57BL/6J animals were homogenised in lysis buffer B (20 mM MOPS, pH 7.4, 10% glycerol, 0.1% CHAPS, 2 mM EDTA, 1 mM DTT, and a protease inhibitor cocktail) using a Polytron homogeniser (Kinematica). After homogenization, CHAPS was added to a final concentration of 1%, and the homogenates were incubated at 4°C with agitation for 15 min, followed by centrifugation at 10,000*g* for 30 min. The supernatant was filtered and loaded onto a TSK-GEL SuperQ-5PW (7.5×75 mm, TOSOH) anion-exchange column pre-equilibrated with Column Buffer A, which consists of 20 mM MOPS (pH 7.4), 10% glycerol, and 2 mM EDTA. After being washed with column buffer A, the proteins were eluted with a linear gradient of NaCl (0–1 M over 60 min) at a flow rate of 0.5 ml min^{-1}. The fractions (0.5 ml each) were collected, and a 50-μl aliquot of each fraction was analysed using an *in vitro* kinase assay, as described below. These hot samples were prepared in the presence of 0.3% TFA (trifluoroacetic acid), 0.1% OG (*n*-octyl-β-D-thioglucopyranoside), and 20% acetonitrile and loaded onto a 5Ph-AR-300 (4.6×250 mm, Nacalai Tesque)

DOI: 10.1038/ncb2060

reverse-phase HPLC column pre-equilibrated with column buffer B, which consists of 0.1% TFA and 0.1% OG. After being washed with column buffer B, the proteins were eluted with a linear gradient of acetonitrile (30–50% over 60 min) at a flow rate of 0.5 ml min^{-1}. Each fraction was analysed by SDS–PAGE and visualized by silver staining and autoradiography. After the purification was scaled up, the procedures described above were again performed using cold ATP instead of γ-^{32}P ATP. Target cold bands matching the hot bands were excised from the gel and analysed using MALDI-Qq-TOF MS/MS.

***In vitro* kinase assay.** Fraction samples were preheated at 65°C for 20 min and incubated with KD or WT AMPK–cFlag in the presence of 0.2 mM AMP, 0.8 mM $MgCl_2$, and 5 μCi of γ-^{32}P ATP (GE Healthcare Bio-Science) at 30°C for 60 min and ultrafiltrated in PBS containing 0.1% SDS using a Nanosep 10K Device (Pall Life Science). Each fraction sample was analysed by SDS–PAGE and visualised by AR. Recombinant Flag-tagged or GST-fused CLIP proteins were also incubated with KD or WT AMPK–cFlag, as described above. Each protein was analysed by SDS–PAGE and either visualized by Coomassie brilliant blue or autoradiography, or examined by immunoblotting. For the CLIP-170 phosphorylation assay, purified GST–CLIP-170 was incubated with PKA or PKC or AMPK purified from rat liver in the presence of 0.2 mM AMP (AMPK), 10 mM $MgCl_2$, and 5 μCi of γ-^{32}P ATP at 30°C for 60 min, analysed by SDS–PAGE and visualised by autoradiography.

Phosphorylation assay. Phosphorylation assays were carried out at 30°C in a reaction volume of 10 μl containing Tris-HCl (20 mM, pH 7.4), glycerol (10%), NaCl (0.3 mM), AMP (0.2 mM), $MgCl_2$ (0.8 mM), γ-^{32}P ATP (10 μCi, 1.7 pmol), AMPK purified from rat liver (0.2 units), and GST-fused CLIP-170 protein. After 60 min, reactions were terminated by the addition of SDS-stop solution, and the CLIP-170 protein and a known concentration of BSA as a volume control were analysed by SDS–PAGE followed by Coomassie brilliant blue staining. From the intensity of each BSA band, the amount of CLIP-170 protein was estimated. With the autoradiogram as a guide, the ^{32}P-labelled CLIP-170 protein was excised from the gel. Its radioactivity and several known concentrations of γ-^{32}P ATP were measured using a Cerenkov counter. The moles of CLIP-170 protein used in this assay and mole of ^{32}P incorporated into the CLIP-170 protein were estimated based on a standard curve.

Phospho-amino acid analysis. CLIP-170-cFlag was incubated with AMPK–cFlag in the presence of γ-^{32}P ATP, as described above. The reaction samples were separated by SDS–PAGE, stained with Coomassie brilliant blue, and visualised by AR. The radiolabelled band was excised from the gel and digested with trypsin. The hydrolysate was dried and resuspended in 5% TFA and 50% acetonitrile containing phospho-amino acid standards and then spotted onto thin-layer cellulose plates. Electrophoresis was performed using pH 1.9 buffer (0.22% formic acid and 7.8% acetic acid) for the first dimension and pH 3.5 buffer (5% acetic acid, 0.5% pyridine, and 0.5 mM EDTA) for the second dimension. The standards were then labelled with ninhydrin, and the plates were analysed by autoradiography.

Biochemical analysis. Protein expression levels in Vero cells were investigated as follows. To inhibit AMPK, cells were serum-starved for 5 h; incubated with 0.2% DMSO, Compound C (20 μM) or AICAR (2 mM) for 10 min; lysed in lysis buffer A; and agitated at 4°C for 15 min. After centrifugation, the supernatants were analysed by SDS–PAGE and examined by immunoblotting. For the phosphatase treatment, cells were lysed in lysis buffer C (50 mM Tris-HCl, pH 7.5, 0.01% Brij 35, 0.1 M NaCl, 0.1 mM EGTA, 2 mM DTT, 2 mM $MnCl_2$, protease inhibitor cocktail, 50 mM β-glycerophosphate, 25 mM NaF and 1 mM Na_3VO_4) and agitated at 4°C for 15 min. After centrifugation, the supernatants were incubated at 30°C for 30 min in the presence of either 20 units μl^{-1} λ protein phosphatase (New England Biolabs) or 0.5 mM EDTA.

Immunocytochemistry and fluorescence imaging. Vero cells and Vero cells stably or transiently expressing CLIP-170–EGFP were seeded on a collagen-coated 35-mm glass dishes (Asahi Techno Glass Corporation). When we stained cells with a detyrosinated tubulin antibody, Vero cells were seeded on a polylysine coated glass dishes to avoid integrin-dependent cell contact. Cells were washed once with warm PBS and fixed with 100% methanol for 10 min at –20°C, followed by 1% paraformaldehyde for 5 min at room temperature. Next, the cells were permeabilized with 0.01% Triton X-100 in PBS for 5 min at room temperature and then immunostained with anti-CLIP-170 C, anti-p-CLIP-170, anti-paxillin, anti-α-tubulin and anti-detyrosinated tubulin antibodies and DAPI for 1 h. For the staining with Alexa Fluor 555-conjugated phalloidin, cells were fixed with 3% paraformaldehyde at room temperature for 5 min. For secondary reactions, each species-matched Alexa 350-, 488- or 568-labelled secondary antibody was used. Fluorescence images of EGFP, Alexa 350, Alexa 488, Alexa 555, and Alexa 568 were recorded with an Olympus IX-81 inverted fluorescence microscope (Olympus) equipped with a cooled CCD CoolSNAP-HQ camera (Roper Scientific) using a PLAPO 60X or 100X (Olympus) oil immersion objective lens. All intensity profiles were analysed in MetaMorph 7.1.3.0 software (MDS Analytical Technologies). Line intensity analysis was performed as described by Komarova *et al.*[25]. Briefly, for the linescan analysis, the intensity profiles along 1 pixel depth line at the microtubule tips were analysed. To estimate the amount of CLIP-170 bound either to the outermost microtubule tips within a box of four pixels (within a 0.129-μm square box) on a side (outer tip) or to the entire microtubule tips within a rectangle covering the entire positively stained tip (total bound), integrated fluorescence intensity at each area was measured for each channel after external background of the same area was subtracted. To quantify the amount of stabilized and total tubulin, the integrated fluorescence intensity stained with a detyrosinated tubulin antibody or an α-tubulin antibody was measured throughout whole cell with background subtraction and divided by the cell area. To measure the paxillin-positive area, lines at every fluorescent border were detected automatically, and each area enclosed by these lines was calculated using WinROOF Ver.6.0 (MITANI Corporation).

Time-lapse imaging and tracking. Vero cells and Vero cells stably or transiently expressing CLIP-170–EGFP were seeded on a collagen-coated 35-mm glass dish at a density of 4×10^4 cm^{-2}, starved for 5 h, and stimulated as indicated in the figures. The fluorescence images were recorded with an Olympus IX-81 inverted fluorescence microscope (Olympus) equipped with a cooled CCD CoolSNAP-HQ camera (Roper Scientific) using a PLAPO ×60 or ×100 (Olympus) oil immersion objective lens controlled by MetaMorph version 7.1.3.0. An EGFP image was obtained every second through a U-MNIBA2 filter (Olympus), which had a 470–495 excitation filter and a 510–550 emission filter. For fluorescence intensity plots of CLIP-170–EGFP, fluorescent images were acquired as described by Komarova *et al.*[25]. Briefly, time-lapse series of 30 images were acquired with a 500-msec interval using stream acquisition mode. CLIP-170 kinetics were analysed on 16-bit depth images after subtraction of the external background. We measured the fluorescence intensity values within the line of 1 pixel in width along the CLIP-170–EGFP tracks over time. We determined the beginning of a comet as the point at which fluorescence intensity showed a rapid rise and the end of a comet as the point at which fluorescence intensity reached baseline. Differential interference contrast (DIC) images were obtained every 10 min. MetaMorph was used to convert a series of time lapse images to video format and obtain tracking images.

Scratch assay. Vero cells were plated on a collagen-coated dish at a density of 2×10^4 cm^{-2} and transiently transfected with WT, S311A, or S311D CLIP-170–EGFP using Lipofectamine 2000. One hour later, siRNA was administered using the same procedure. After 40 h, cells were plated on a collagen-coated 35-mm glass dish at a density of 8×10^4 cm^{-2}. When we stained cells with a detyrosinated tubulin antibody, Vero cells were seeded on a polylysine coated glass dishes. After 8 h, a scratch line was made with a p200 pipette tip, and the dishes were washed once with fresh medium. Repeated observations of the edge of the same scratched lesion were performed. Either 0.2% DMSO (control) or Compound C (20 μM) was administered every 2 h, and the medium was replaced every 4 h. After 12 h, the cells were fixed and immunostained with a γ-tubulin antibody, as described above. For the cell polarity analysis, the angles (θ) of each cell to the scratched line were measured. First, we drew line A from the point stained with a γ-tubulin antibody to the centre of the nucleus. Next, we drew line B from the centre of the nucleus to the scratched line. The angles (θ) between lines A and B were determined. The distance of gap closure was calculated as the total distance of the gap closed over 12 h. Also, the numbers of cells in the first two layers from the edge that were perpendicular with respect to their migration direction were calculated.

Cell migration assay. Vero cells were prepared as described for the scratch assay. Cells were plated on a collagen-coated 35-mm glass dish at a density of 5×10^3 cm^{-2}. After 3 h, DIC images were recorded every 10 min for 12 h with an Olympus IX-81 inverted fluorescence microscope equipped with an ONICS stage top incubator sys-

tem and an INUG2 temperature and CO_2 control unit (Tokai Hit). RFP images were also recorded at the same time to assess whether the siRNA duplex was effectively delivered into each cell by the co-transfection of control siRNA labelled with Alexa Fluor 546 (Qiagen) and siRNA targeting for AMPK. To determine cell trajectories, the centrioles of the cell nuclei were tracked throughout time-lapse movies, and we made migration tracking images using MetaMorph 7.1.3.0 software. Migration speed was expressed as the average of each migration speed obtained every 10 min.

Statistical analyses. Box and whisker plots show the entire population. Other data are expressed as means ± s.e.m. The two-tailed Student's *t*-test was used to analyse differences between two groups. Differences among multiple groups were compared by one-way ANOVA, followed by a post hoc comparison using the Dunnett method with JMP 8.0.1 software (SAS Institute). $P < 0.01$ was considered statistically significant.

23. Fukata, M. *et al.* Rac1 and Cdc42 capture microtubules through IQGAP1 and CLIP-170. *Cell* **109,** 873–885 (2002).
24. Palazzo, A. F. *et al.* Cdc42, dynein, and dynactin regulate MTOC reorientation independent of Rho-regulated microtubule stabilization. *Curr. Biol.* **11,** 1536–1541 (2001).
25. Komarova, Y. *et al.* EB1 and EB3 control CLIP dissociation from the ends of growing microtubules. *Mol. Biol. Cell* **16,** 5334–5345 (2005).

nature cell biology

DOI: 10.1038/ncb2060

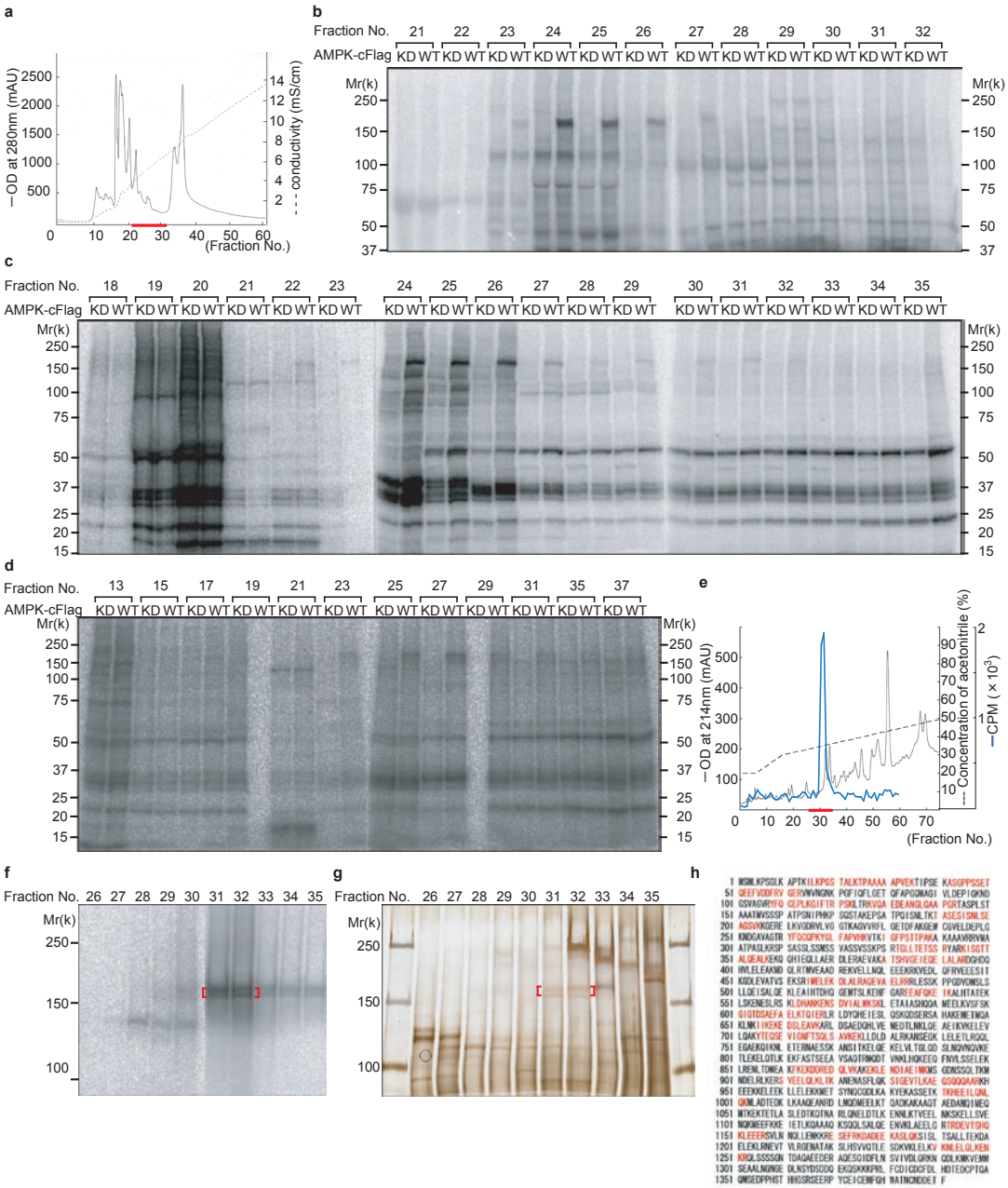

Figure S1 Screening of AMPK substrate in various organs. (**a**) A graphic chart of the fractions acquired from homogenised mouse heart using an anion exchange column with an NaCl concentration gradient (dotted line). The solid line represents the optical density (OD) of each sample. Further analysis was performed using fractionated samples, indicated by the red line. (**b-d**) In vitro kinase reaction. A wide range of fractionated samples from mouse heart (**b**), placenta (**c**), and liver (**d**) were incubated with recombinant kinase-dead (KD) or wild-type (WT) AMPK in the presence of [γ-32P] ATP, separated by SDS-PAGE, and visualised by autoradiography. A 32P-incorporated ~170 kDa polypeptide (p170) was detected in fractions treated with WT AMPK but not in fractions treated with KD AMPK (fractions 23 to 27 in **b**). (**e**) A graphic chart of the fractions containing AMPK-induced 32P-incorporated proteins from mouse heart using a reverse-phase high-performance liquid chromatography (HPLC) column with an acetonitrile concentration gradient (dotted line). The solid black line represents the optical density (OD) of each sample. The radioactivity of each refractionated sample was measured using a Cerenkov counter (blue line). Further analysis was performed using refractionated samples, indicated by the red line. (**f, g**) Images obtained by autoradiography (**f**) and silver staining (**g**) of samples that were refractionated by reverse-phase HPLC. Red brackets denote p170 incorporated 32P by AMPK. (**h**) Amino acid sequence of CLIP-170. Sequence analysis by MALDI-Qq-TOF MS/MS revealed p170 to be CLIP-170. Matching amino acids are shown in red letters.

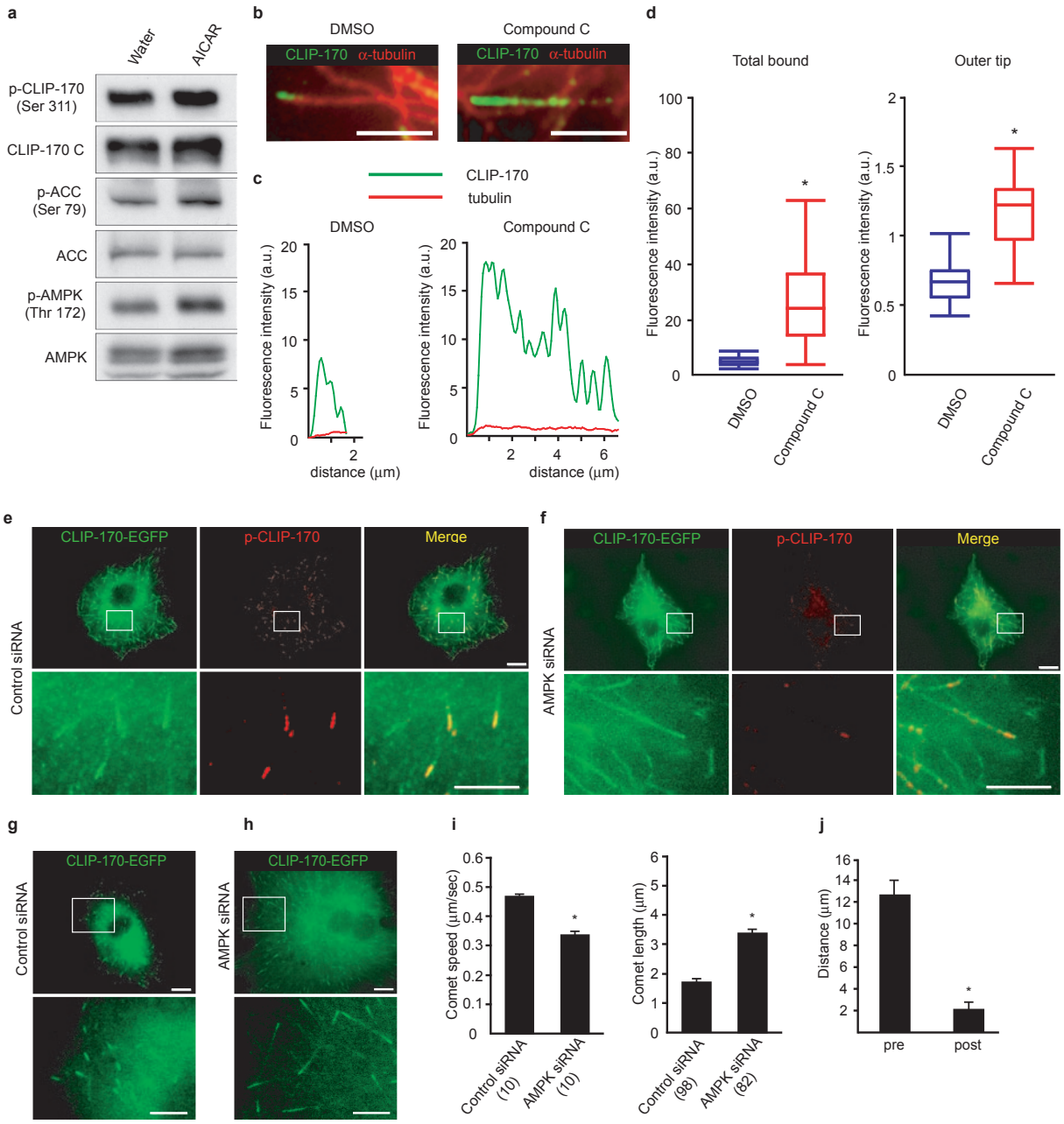

Figure S2 (**a**) Lysates from Vero cells treated with 2 mM of AICAR were analysed for the phosphorylation of CLIP-170, ACC, and AMPK. (**b**) Images of Vero cells that were immunostained with both a CLIP-170 C antibody and an α-tubulin antibody after DMSO (left) or Compound C (right) treatment. The scale bars represent 3 μm. (**c**) Linescan analysis along the staining area by a CLIP-170 C (green) and a α-tubulin (red) antibody corresponding to figure (**b**), which shows the distribution of CLIP-170 treated with DMSO (left) or Compound C (right). (**d**) Box and whisker plots of the intensity of CLIP-170 bound to the whole tip (left) or to its outer part (right) after treatment with DMSO (blue) or Compound C (red). *n*=30, *p<0.01 versus DMSO. (**e, f**) Immunostained images of Vero cells stably expressing WT CLIP-170-EGFP (GFP image, each shown in the left) and treated with control siRNA (**e**) and siRNA targeting both AMPKα1 and α2 (**f**). These cells were stained with a p-CLIP-170 antibody (centre). The merged images are shown on the right. The boxed regions in the panels are enlarged below each panel. The scale bars represent 10 μm (upper row) and 5 μm (lower row). (**g, h**) GFP images of Vero cells stably expressing CLIP-170-EGFP treated with control siRNA (**g**) or siRNA targeting both AMPKα1 and α2 (**h**). The white boxed regions in the panels are enlarged below each panel. The scale bars represent 10 μm (**g**, **h** upper row) and 5 μm (enlarged images of **g**, **h**). (**i**) Bar graphs showing the speed (left) and length (right) of a single comet of cells treated with control siRNA or siRNA targeting both AMPKα1 and α2. Values are means ± s.e.m. *n* are given in parentheses. *p<0.01 versus control siRNA. (**j**) Bar graphs showing the shortening distance measured for 30 microtubules before and after Compound C treatment. Values represent means ± s.e.m. *p<0.01 versus pre.

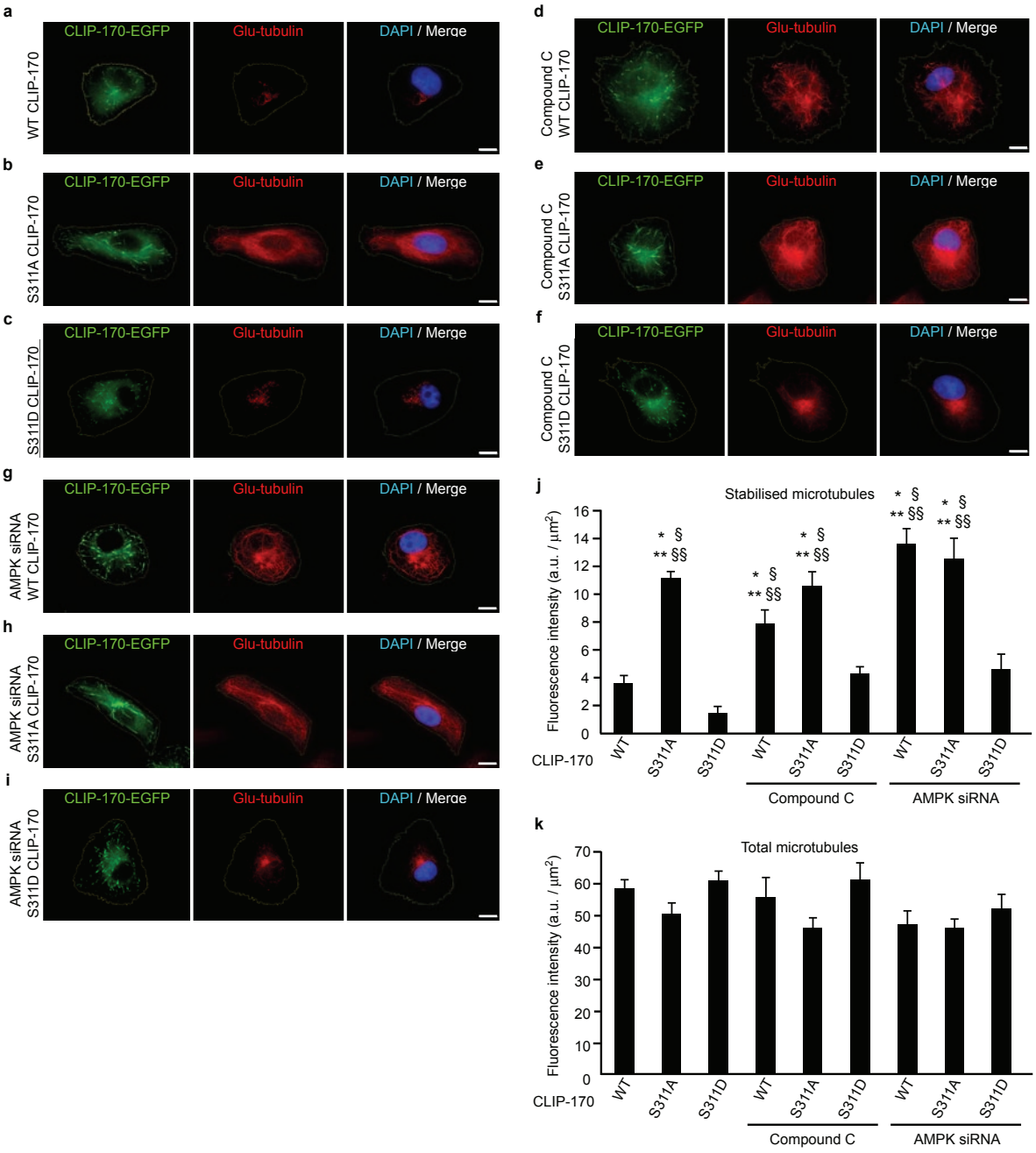

Figure S3 Loss of CLIP-170 phosphorylation increases stabilised microtubules. (**a-c**) Immunostained images of Vero cells transiently expressing WT (**a**), S311A (**b**) and S311D (**c**) CLIP-170-EGFP (GFP image, each left, green). These cells were stained with a detyrosinated (Glu) tubulin antibody (each centre, red) to visualise stable microtubules. (**d-f**) Immunostained images of Vero cells transiently expressing WT (**d**), S311A (**e**) and S311D (**f**) CLIP-170-EGFP (GFP image, each left, green) treated with Compound C. These cells were also stained with a detyrosinated (Glu) tubulin antibody (each centre, red). (**g-i**) Immunostained images of Vero cells expressing WT (**g**), S311A (**h**) and S311D (**i**) CLIP-170-EGFP (GFP image, each left, green) treated with siRNA targeting both AMPKα1 and α2. These cells were also stained with a detyrosinated (Glu) tubulin antibody (each centre, red). DAPI stained nucleus (blue). Yellow dotted line indicates border zone of cells and fluorescence intensity in this area was measured. The scale bars represent 10 μm. (**j, k**) Bar graphs showing the amount of stabilised microtubules (**j**, detyrosinated tubulin antibody positive) and total microtubules (**k**, α-tubulin antibody positive) in various conditions. Y axis indicates fluorescence intensity divided by the area size of cells. Values are means ± s.e.m. *n*=10 for each group. *p<0.01 versus WT CLIP-170. **p<0.01 versus S311D CLIP-170. §p<0.01 versus S311D CLIP-170 with Compound C. §§p<0.01 versus S311D CLIP-170 with AMPK siRNA.

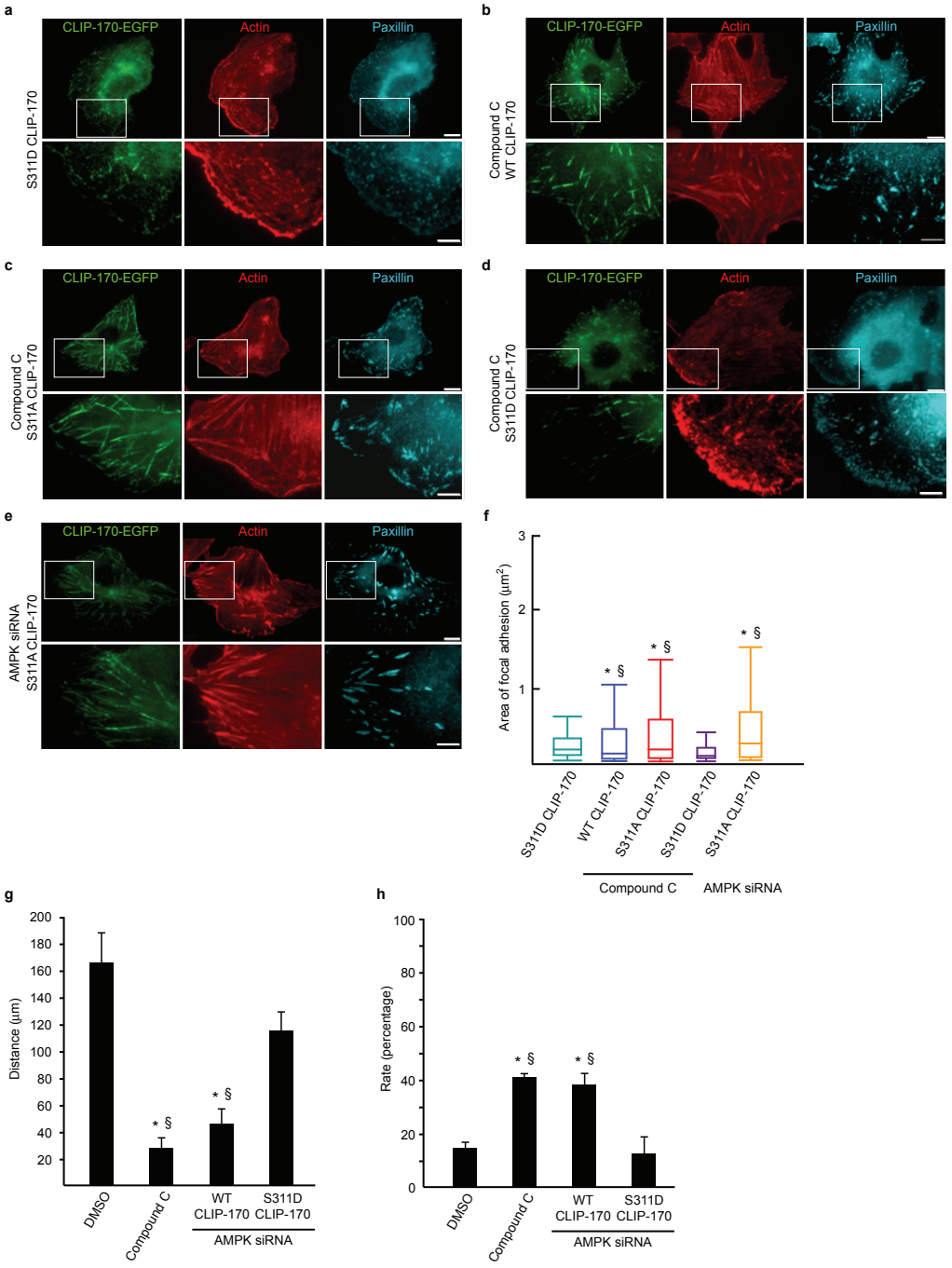

Figure S4 Loss of CLIP-170 phosphorylation increases the size of focal adhesion. (**a**) Immunostained images of Vero cells transiently expressing S311D CLIP-170-EGFP (GFP image, left). These cells were stained with fluorescein-conjugated phalloidin (centre) and a paxillin antibody (right) to visualise actin microfilaments and focal adhesions, respectively. (**b-d**) Immunostained images of Vero cells transiently expressing WT (**b**), S311A (**c**) and S311D (**d**) CLIP-170-EGFP (GFP image, left) treated with Compound C. These cells were also stained with fluorescein-conjugated phalloidin (centre) and a paxillin antibody (right). (**e**) Immunostained images of Vero cells transiently expressing S311A CLIP-170-EGFP (GFP image, left) treated with siRNA targeting both AMPKα1 and α2. These cells were also stained with fluorescein-conjugated phalloidin (centre) and a paxillin antibody (right). The white boxed regions in the panels are enlarged below each panel. The scale bars represent 10 μm (**a-e**, upper row) and 5 μm (**a-e**, bottom row). (**f**) Box and whisker plots of the area stained with a paxillin antibody showing the 25th percentile (bottom line of each box), median (middle line of each box), 75th percentile (top line of each box), and the 5th and 95th percentiles (each whisker). *n*=10 for each group. *p<0.01 versus S311D CLIP-170. §p<0.01 versus S311D CLIP-170 with Compound C. (**g**) Bar graph showing the distance of the gap closed 12 h after scratch. The cells were treated by either repeated administration of DMSO or Compound C, or transfected with WT or S311D CLIP-170 and siRNA targeting both AMPKα1and α2. (**h**) Bar graphs showing the rate of cells that are perpendicular with respect to their migration direction in the first two layers of the leading cells. Values are means ± s.e.m. of triplicates. *p<0.01 versus DMSO. §p<0.01 versus S311D CLIP-170 with siRNA for AMPK.

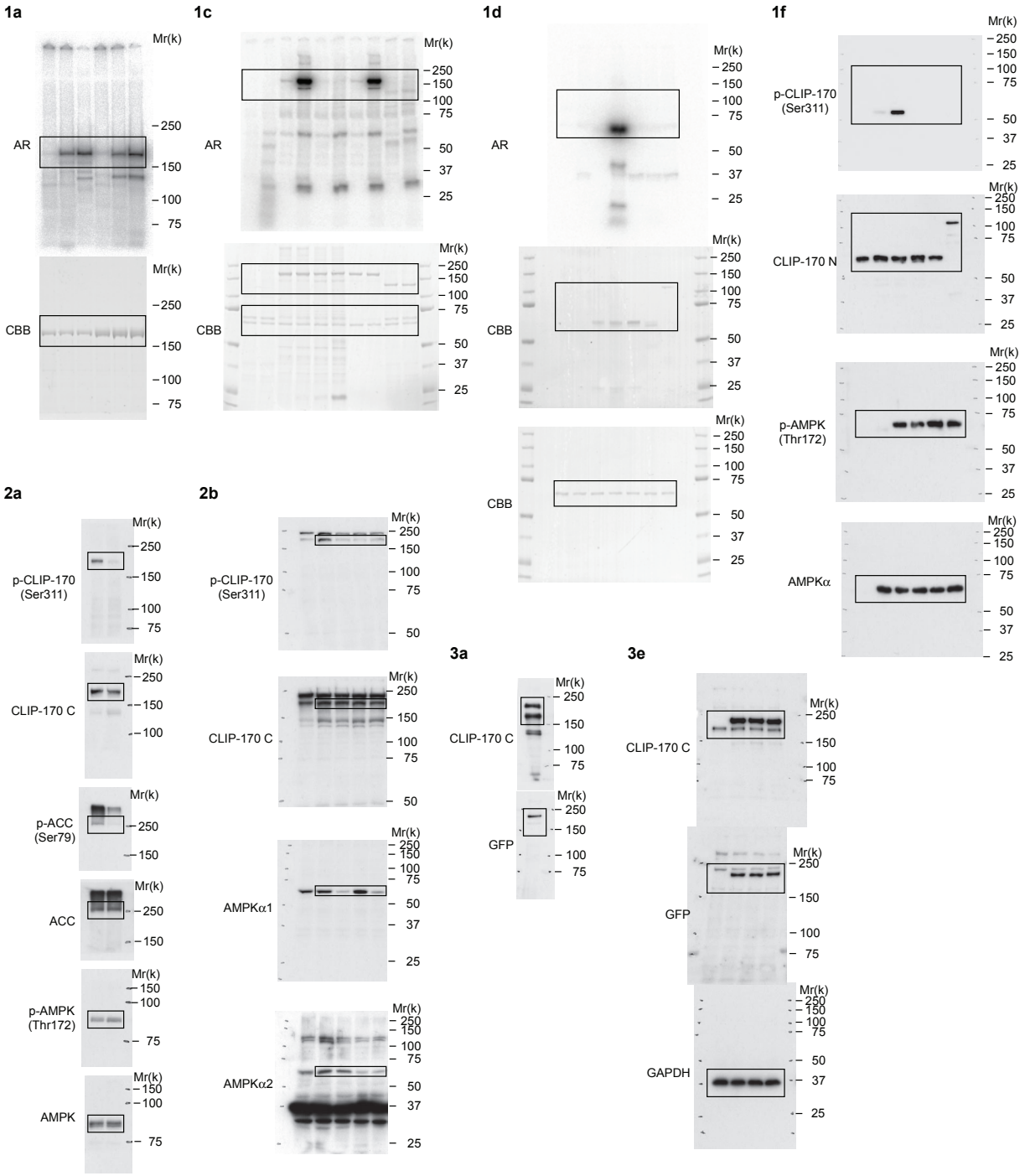

Figure S5 Uncropped versions of the immunoblots shown in the main figures.

Table S1 Properties of comet dynamics on microtubules in Vero cells transiently expressing different CLIP-170-EGFP constructs treated with various conditions. Cells were treated with compound C for 10 min or transfected with siRNA targeting both AMPKα1 and α2. Values are means ± s.e.m. *p<0.01 versus WT CLIP-170 before Compound C. **p<0.01 versus S311D CLIP-170 before Compound C. ***p<0.01 versus S311D CLIP-170 after Compound C. §p<0.01 versus WT CLIP-170 with siRNA for AMPK. §§p<0.01 versus S311D CLIP-170 with siRNA for AMPK. WT, wild type.

treatment	CLIP-170	comet speed (μm/sec)	comet length (μm)
Before Compound C	WT	0.48 ± 0.01 (n=10)	1.80 ± 0.05 (n=132)
	S311A	0.26 ± 0.02 (n=10) * **	3.20 ± 0.11 (n=109) * **
	S311D	0.54 ± 0.01 (n=10)	1.56 ± 0.04 (n=99)
After Compound C	WT	0.34 ± 0.01 (n=10) * ***	3.68 ± 0.09 (n=115) * ***
	S311A	0.24 ± 0.03 (n=10) * ***	3.42 ± 0.11 (n=108) * ***
	S311D	0.48 ± 0.02 (n=10)	1.62 ± 0.05 (n=91)
AMPK siRNA	WT	0.34 ± 0.02 (n=10)	3.29 ± 0.15 (n=92)
	S311A	0.22 ± 0.02 (n=10) § §§	3.32 ± 0.12 (n=87) § §§
	S311D	0.50 ± 0.01 (n=10)	1.49 ± 0.03 (n=127)

Supplementary Movie Legends

Movie S1 Time lapse imaging of a cell stably expressing WT CLIP-170-EGFP and treated with DMSO (control). An EGFP image was obtained every second for 1 min at baseline and then 2 min, 10 min, and 20 min after administration of DMSO. The scale bar represents 10 μm.

Movie S2 Time lapse imaging of a cell stably expressing WT CLIP-170-EGFP and treated with Compound C. An EGFP image was obtained every second for 1 min at baseline and then 2 min, 10 min, and 20 min after administration of Compound C. The scale bar represents 10 μm.

Movie S3 Time lapse imaging of a cell stably expressing WT CLIP-170-EGFP and treated with siRNA targeting both AMPKα1 and α2. An EGFP image was obtained every second for 1 min. The scale bar represents 10 μm.

Movie S4 Time lapse imaging of a cell transiently expressing S311A CLIP-170-EGFP. An EGFP image was obtained every second for 1 min. The scale bar represents 10 μm.

Movie S5 Time lapse imaging of a cell transiently expressing S311D CLIP-170-EGFP. An EGFP image was obtained every second for 1 min. The scale bar represents 10 μm.

Movie S6 Time lapse imaging of a cell transiently expressing WT (upper half) or S311D (lower half) CLIP-170-EGFP treated with control siRNA (left) or siRNA targeting both AMPKα1 and α2 (right). An EGFP image was obtained every second for 1 min. The scale bar represents 10 μm.

Movie S7 Time lapse imaging of a cell stably expressing tubulin-EGFP before (left) and 10 minutes after (right) Compound C treatment. An EGFP image was obtained every second for 2 min. The scale bar represents 10 μm.

Movie S8 Cell migration assay. Time lapse imaging of cells transiently expressing WT CLIP-170 (upper left panel), S311A CLIP-170 (upper right panel), WT CLIP-170 treated with siRNA targeting both AMPKα1 and α2 (lower left panel) and S311D CLIP-170 treated with siRNA targeting both AMPKα1 and α2 (lower right panel). A DIC image (upper half), and a merged image of DIC and RFP (lower half) were obtained every 10 min for 12 h. An RFP image indicates effective delivery of siRNA for AMPK into each cell.